

Full-Length Research Article

A Comparative Study of Skull Shape Variations in *Eidolon helvum* (African Fruit Bat) from Two Geographical Locations in Nigeria

*Igado, O. O. and Joannis, J. S

Department of Veterinary Anatomy, University of Ibadan, Nigeria

Summary: The shape and size of a skull provides insight into the age, breed and gender of the animal. Skull shape variations have been reported in different animals, with some theories linking these variations to evolution and/or migration. This study assessed the variations observed in the skull shape, size and gross morphometrics of two groups of the *Eidolon helvum* obtained from two geographical regions in Nigeria (south and north). All skulls were rostro-caudally elongated, having a dolichocephalic appearance. The skulls from the north had a distinct dome shape, with a more prominent zygomatic process, absence of a 'diastema' and an extra upper molar, while the southern skulls showed a more dorsally flattened skull and a less prominent zygomatic process. The shape of the sagittal crest was different in the two groups, while there was the presence of an accessory infraorbital foramen in some of the southern skulls. The southern skulls lacked the palatine foramen. The lacrimal foramen was observed to be more caudally placed in the southern skulls. Values for most linear measurements were higher in the northern skulls, although statistically significant difference was not present in all. The value for the neurocranial volume was considerably higher in the northern skulls (4.41 ± 0.28 mls) relative to the southern skulls (2.0 ± 0.27 mls). Statistically significant differences were not observed between males and females (within regions). Data obtained from this study may find application in evolution and migration studies, wildlife medicine and surgery and comparative and forensic anatomy.

Keywords: Anthropometry; clinical implications; craniofacial osteometrics; megachiroptera; wildlife and comparative anatomy

©Physiological Society of Nigeria

*Address for correspondence: E-mail: mayowaigado@yahoo.com; oo.igado@mail1.ui.edu.ng; Tel: +234-8035790102

Manuscript received- November- 2021; Accepted- April, 2022

DOI: <https://doi.org/10.54548/njps.v37i1.13>

INTRODUCTION

Craniometry is an anthropometric parameter that involves the measurement of cranial features to categorise them according to race, intelligence, etc (Durbar, 2014). By extension, cranial osteometrics (measurement of bones of the skull) has proven to be invaluable in identifying species, breeds and gender, providing baseline anatomical data and finding usefulness in comparative anatomy and forensics. In recent years, there has been an increasing report in animals, for example, goats (Olopade and Onwuka, 2004), bats (Bullen and Mckenzie, 2008), and dogs (Igado, 2017; Janeczek *et al.*, 2008; Onar and Günes, 2003).

This study focuses on the variation of the skull shape, size, general arrangement of some sutures and gross morphometrics of the *Eidolon helvum* (the straw-coloured fruit bat), obtained from two different geographic locations (south and north) in Nigeria.

In Africa, the *E helvum* is reputed to be the most conspicuous megachiroptera (large bats), it is widely distributed throughout sub-Saharan Africa, and is reputed to be the most hunted for bush meat among all bat species in West Africa (Gibson *et al.*, 2021; Richter and Cumming, 2006). It is the second largest, is fruit-eating and also bears unique morphological and ecological characteristics. It is however a poorly diversified genus (Juste *et al.*, 2000),

having only the species *E helvum*. It belongs to the Order Chiroptera, Suborder Megachiroptera, Family Pteropodidae, Genus *Eidolon* (DeFrees and Wilson, 1988). It is the only known flying mammal, with an average body weight of 225 ± 33 g and average wing span of 76 ± 7 cm. They are reputed to be of economic importance (pollination), economic waste (destruction of fruits) and of public health importance (transmission of the rabies virus) (Balthazary *et al.*, 2007).

Being highly diversified, having over 1,400 species, bats have been reported to have significant variation in ecology and morphology, and so offer myriads of opportunities for studies (Brokaw and Smotherman, 2020) involving understanding the correlations between morphology, ecology, evolution and adaptability.

This study of the variation in the skull shape and characteristics of the *E helvum* may play a role in better understanding the evolution of the frugivorous bats, while also finding application in the field of wildlife craniofacial/maxillofacial applied anatomy.

MATERIALS AND METHODS

Ethical considerations: Ethical approval for this study was obtained from the Ethical Committee of the Faculty of Veterinary Medicine, University of Ibadan, Nigeria, Ethical

code number 'ethic/12/13/03'. All procedures followed the Guide for the care and use of experimental animals, according to guidelines by the National Institute of Health (NIH), USA and the Animal Care Use and Research Ethics Committee (ACUREC), University of Ibadan, Nigeria. All bats were handled humanely, to avoid undue stress or pain to them.

Trapping of bats and sacrifice: A total of nineteen adults (10 males and 9 females) were used for this study. Bats were obtained from two geographical locations in Nigeria – 4 males and 3 females from Pandam Game Reserve, Qua'an Pan Local Government Area, Plateau State (Northern Nigeria) and 3 males and 3 females from forests and roosting sites in Ibadan, Oyo State (Southern Nigeria). An additional 6 skulls (3 males and 3 females) obtained previously from *E. helvum* from the same roosting sites in Ibadan were added to the specimens, bringing the total number of the southern skulls to 12 (6 males, 6 females). A larger number of this wildlife could not be used for this study for ethical reasons (especially those collected from the Game Reserve), even though the *E. helvum* are currently not on the list of threatened animals. Using Google map, the geographical coordinates of Qua'an Pan Local Government Area was 8°48'N 9°09'E, while that of Ibadan was 7°23'47"N 3°55'0"E. The bats were captured humanely using mist nets and transported to the Research Laboratory in cages. Bats were certified to be adults using the weight according to previous reports (Richter and Cumming, 2006), and weights were determined using a digital kitchen weighing scale (Electronic Kitchen Scale, Camry® EK5350, China). All subjects used for this study had the typical orange/yellowish coloured ventral aspect peculiar to the *E. helvum*.

They were anaesthetized with ketamine HCl at 50 mg/kg and xylazine 10 mg/kg, administered intramuscularly in the pectoral muscle. This dose was a modification from a previous report in bats (Sohayati *et al.*, 2008). After ascertaining that the bats were deceased (lack of response to strong tactile stimuli and cessation of respiration and heart-beat), they were eviscerated, skinned and all muscles were removed as much as possible. All bones were left intact. Animals were tagged individually for easy identification.

Cold water maceration: The heads were separated from the bodies at the atlanto-occipital junction, and macerated individually in labelled plastic containers. The skulls were macerated using the cold-water maceration method previously described (Igado and Ade-Julius, 2018). The skulls were placed in individual plastic containers with lids, in water solution containing 5% sodium hydroxide (NaOH) pellets for 5 – 9 days at room temperature. This was done to remove the remaining muscles and ligaments still attached to the bone. The water solution was changed during the duration of time of maceration. Then the skulls were rinsed to remove any soft tissue and then transferred to a water solution containing 4.2 % sodium hypochlorite overnight. The skulls were again rinsed in clean water and then left in the sun to air-dry.

Linear morphometry: A total of fifty-two (52) parameters were measured on each skull (Figures 1 – 14). Some of the parameters measured were adapted from previous methods and definitions (Igado, 2017; Igado and Ekeolu, 2014; Onar,

1999). Nomenclatures were derived from veterinary anatomy texts (Getty, 1975; Singh, 2017). Measurements were determined with the aid of a digital vernier calliper (Neiko®, sensitivity of 0.01mm, Germany), centimetre rule, mathematical dividers and compass to the nearest 0.01mm. Pictures were obtained using a digital camera (Sony® Cyber-shot, DSC-HX400V, 50x optical zoom, China).

The parameters measured and their landmarks are described below. All measurements were recorded in millimeters (mm), all paired measurements were obtained consistently from the left side e.g. measurements of orbit.

Neurocranial and viscerocranial measurements

1. **Whole skull height (WSH):** This is the total height of the skull; from the highest level of the frontal bone to the base of the mandible.
2. **Whole skull length (WSL):** This is the total length of the skull; from the most rostral aspect of the dental pad to the most caudal aspect of the occipital bone.
3. **Skull height without the mandible (SHWM 1):** Height of the skull, from the highest limit of the frontal bone to the most ventral aspect of the sphenoid bone, below the foramen magnum.
4. **Maximum width of the skull (MWS):** This is the breadth/width of the skull, measured from zygion to zygion (zygomatic bone to zygomatic bone).
5. **Total length of frontal bone (FBL):** From the rostral tip of the bone, where it articulates with the maxilla and nasal bones, to the caudal border where it forms a suture with the parietal bone.
6. **Overall length of the nasal bone (NBL):** From the rostral end of the frontal bone to the rostral tip of the nasal bone.
7. **Length of parietal bone (FNE):** From the fronto-parietal suture to the nuchal eminence.
8. **Length of palate (PAL):** This was measured along the midline, from the most rostral aspect of the incisive bone, to the most rostral aspect of the choanae.
9. **Length of the perpendicular plate of the palatine (UMP):** From the most rostral aspect of the choanae to the suture between/joining the perpendicular plate of the palatine bone and the pterygoid.
10. **Tympanic bulla length (TBL):** From the rostral aspect to the caudal aspect of the bulla.
11. **Width of the tympanic bulla (TBW):** From one lateral aspect of the bulla to the other lateral aspect.
12. **Orbital height/vertical diameter (OVD):** Height of the orbit, from the ventral aspect of the orbital rim in a vertical line to the dorsal aspect of the rim.
13. **Orbital width/horizontal diameter (OHD):** From the limit of the zygomatic process of the frontal bone to the median canthus of the orbit.
14. **Orbital index:** $\left(\frac{\text{orbital height}-\text{OVD}}{\text{orbital width}-\text{OHD}}\right) \times 100$
15. **Cephalic index:** $\left(\frac{\text{skull width}-\text{MWS}}{\text{skull length}-\text{WSL}}\right) \times 100$
16. **Occipital height (OCH):** Nuchal crest to the lower rim of the foramen magnum.
17. **Maximum width of the occipital condyles (OCW):** Maximum width or distance, from the lateral aspect of one occipital condyle to the lateral aspect of the other occipital condyle.
18. **Neurocranial volume (NCV):** Cotton wool was used to block all the foramina of the intact skull; fine grains were then poured into the neurocranium via the foramen magnum until filled up. The grains were emptied into a measuring cylinder and volume determined.
19. **Length of zygomatic process of frontal bone (LPO):** This was measured from the origin of the zygomatic process on the frontal bone, to its most lateral limit.

20. **Zygomatic process to zygomatic process (POPO):** This was measured from the most lateral limit of one zygomatic process of the frontal bone to the most lateral limit of the other process.
21. Vertical distance from the most lateral limit of zygomatic process to zygomatic bone (POZB).
22. Distance from the rostral tip of the nasal bone to the rostral tip of the incisive bone (NIL)

Mandibular measurements

23. **Length of the mandibular bone (MDL):** From the most rostral point of the dental bone to the caudal limit of the mandibular condyle.
24. Length of the lower jaw from the most rostral point of the dental bone to the most caudal projection of the coronoid process (MDL-1)
25. Length of the lower jaw from the most rostral point of the dental bone to the most caudal projection of the mandibular condyle (condylar process) (MDL-2)
26. Length of the lower jaw, from the most rostral point of the dental bone to the most caudal projection of the angular process (MDL-3)
27. **Height of the mandibular symphysis (HSPH):** This was measured as the vertical distance from the dorsal to the ventral limits of the mandibular symphysis
28. **Length of the mandibular symphysis (LSPH):** This was measured from the rostral to the caudal limits of the mandibular symphysis.
29. **Width of the condylar process (WCP):** This was measured from one lateral aspect to the other lateral aspect of the condylar process of the mandible.
30. Distance between the two lower (mandibular) premolars, at the level of the 2nd premolars, measured along the transverse plane (D2P)
31. Distance between the lower (mandibular) 2nd molars, measured along the transverse plane (DLM)
32. Height of the mandibular body between the mid-point of premolar 1 and 2 and the mandibular base (HMP)
33. Thickness of mandible at molar 1 (TM-1)
34. Thickness of the mandible, between the medial and lateral parts of the mandible, caudal to the last molar tooth (TR)
35. Length of the mandible between the cranial and caudal angles (RAM). This was measured as the distance from immediately caudal to the last molar tooth (cranial angle), to the ventral aspect of the angular process (caudal angle).

Foramen diameters and foramen-related measurements: Parameters relating to some foramina which may aid in maxillofacial anaesthesiology (rostrofacial indices). The lacrimal fossa was used as a reference point for some parameters, since the edge of the orbit may be easier to palpate and access in some live patients.

36. **Occipital height without foramen magnum (OCHW):** Nuchal crest to the upper rim of the foramen magnum.
37. **Height of the foramen magnum (FMH):** Maximum height of the foramen magnum, or distance between the dorsal and ventral limits of the foramen magnum.
38. **Width of the foramen magnum (FMW):** Maximum width, between the two lateral limits of the foramen magnum.
39. **Foramen magnum index (FMI):** calculated as $\left(\frac{FMH}{FMW}\right) * 100$, expressed in percentage.
40. Distance between the most medial points of the most rostral left and right mental foramina (RMF)
41. Distance between the alveolar border of the 3rd lower incisor and the most ventral point of the most rostral mental foramen (IRMF)

42. Length along a horizontal line, from the ventral limit of the mandibular foramen to the caudal border of the mandible (MFCB)
43. Length, along a vertical line, from the ventral limit of the middle mental foramen, to the ventral border of the mandibular foramen (MFMF)
44. Length, along a vertical line, from the ventral limit of the mandibular foramen, to the base of the mandible (MFMB)
45. Length along a vertical line, from the ventral limit of the mandibular foramen, to the most dorsal aspect of the coronoid process (MFCP)
46. Distance between the caudal limit/rim of the lacrimal foramen and the medial canthus of the orbit (IFMO)
47. Distance from the ventral limit of the lacrimal foramen to the alveolar border between the upper 3rd and 4th premolars (IFP).
48. Distance, along a horizontal line, between the caudal rim of the lacrimal foramen and the cranial tip of the facial crest (FCIF)
49. Distance, from the zygomatic arch to the caudal rim of the lacrimal foramen (ZPIF).
50. **Diameter of the lacrimal foramen (DIF):** This was measured vertically, in a straight line, as the distance between the dorsal and ventral limits of the lacrimal foramen.
51. **Diameter of infraorbital foramen (DIC):** This was measured vertically, in a straight line, as the distance between the dorsal and ventral limits of the infraorbital foramen.
52. Distance between the infraorbital foramen and the medial canthus of the orbit/the orbit (ICMC).

Statistical analysis

All data were analysed using the Graphpad prism version 5 software. Statistically significant difference between different group parameters (gender and location) were determined using the Student 't' test. Pearson's correlation was assessed by correlating the whole skull length with other parameters. Statistically significant difference was at $\alpha_{0.05}$.

RESULTS

Linear parameters were measured in millimetres (mm) and recorded as mean \pm standard deviation (S.D.). Morphometric results are presented in Tables 1 and 2, while Pearson's correlation data are presented in Table 3.

General appearance of the skulls: The skulls of the *E. helvum* were rostro-caudally elongated, having a dolichocephalic appearance (Figure 1). All the skulls possessed a bilaterally placed supraorbital foramen, at the cranio-rostral aspect of the beginning of the zygomatic process (Figure 2). The supraorbital foramen led ventrally into a canal (supraorbital canal) which opened into the roof of the orbit. The nasal bone protruded slightly more cranially than the incisive bone. No palatine fissure or inter-incisive canal was present (Figure 3). The paracondylar processes were short, resulting in the skull resting on the occipital condyles.

The lacrimal foramen was external in both skull types. In the northern skulls, it was placed above the 1st and 2nd molar, while in the southern skull, it was placed behind the 2nd molar (dorso-caudal) (Figure 1). The foramen magnum had the typical spherical appearance in all the skulls assessed (Figure 4).

Table 1: Linear morphometric values of skulls of *Eidolon helvum* from Nigeria (north and south regions)

	S/N	Parameters (unit – mm)	Mean ± S.D. (Total) n = 19	(Male) n = 10 Mean ± S.D.	(Female) n = 9; Mean ± S.D.
Neurocranial and viscerocranial measurements	1.	WSH	24.02 ± 2.03	24.21 ± 1.29	23.80 ± 2.85
	2.	WSL	55.42 ± 2.16	55.89 ± 1.30	54.94 ± 2.88
	3.	SHWM1	17.09 ± 3.29	17.29 ± 3.22	16.90 ± 3.73
	4.	MWS	30.77 ± 3.15	30.79 ± 2.50	30.75 ± 4.12
	5.	FBL	18.80 ± 2.42	18.95 ± 3.00	18.62 ± 1.81
	6.	NBL	24.02 ± 3.35	24.35 ± 4.57	23.63 ± 1.29
	7.	FNE	15.79 ± 2.43	15.50 ± 2.45	16.13 ± 2.65
	8.	PAL	31.30 ± 4.05	31.69 ± 4.79	30.84 ± 3.45
	9.	UMP	3.48 ± 1.18	3.38 ± 1.43	3.635 ± 0.86
	10.	TBL	3.60 ± 0.33	3.57 ± 0.254	3.63 ± 0.42
	11.	TBW	2.99 ± 0.27	2.96 ± 0.07	3.04 ± 0.42
	12.	OVD	11.82 ± 1.3220	12.04 ± 1.02	11.54 ± 1.71
	13.	OHD	11.88 ± 0.79	12.05 ± 0.66	11.68 ± 0.97
	14.	Orbital index (%)	101.10 ± 6.44	100.30 ± 5.49	102.10 ± 8.00
	15.	Cephalic index (%)	55.95 ± 5.54	56.00 ± 5.44	55.90 ± 6.28
	16.	OCH	10.90 ± 1.58	11.04 ± 1.55	10.76 ± 1.78
	17.	OCW	9.73 ± 0.90	9.92 ± 1.06	9.54 ± 0.77
	18.	NCV (mls)	3.53 ± 1.24	3.52 ± 1.06	3.55 ± 1.56
	19.	LPO	8.88 ± 2.36	8.96 ± 1.90	8.77 ± 3.06
	20.	POPO	22.95 ± 3.50	23.17 ± 2.50	22.73 ± 4.60
	21.	POZB	5.82 ± 0.46	5.86 ± 0.28	5.77 ± 0.64
	22.	NIL	6.59 ± 0.249	6.64 ± 0.27	6.53 ± 0.23
Mandibular measurements	23.	MDL	44.67 ± 2.57	45.00 ± 2.53	44.29 ± 2.86
	24.	MDL-1	41.58 ± 2.10	42.20 ± 1.27	40.84 ± 2.78
	25.	MDL-2	42.81 ± 3.18	42.89 ± 3.53	42.72 ± 3.12
	26.	MDL-3	41.28 ± 2.48	41.51 ± 2.85	41.01 ± 2.25
	27.	HSPH	4.55 ± 0.45	4.58 ± 0.33	4.52 ± 0.60
	28.	LSPH	6.20 ± 0.84	6.43 ± 0.84	5.92 ± 0.84
	29.	WCP	4.86 ± 0.44	4.86 ± 0.23	4.86 ± 0.64
	30.	D2P	6.88 ± 0.50	6.89 ± 0.57	6.87 ± 0.47
	31.	DLM	13.57 ± 1.72	13.60 ± 1.23	13.55 ± 2.35
	32.	HMP	4.48 ± 0.34	4.53 ± 0.30	4.42 ± 0.42
	33.	TM-1	2.212 ± 0.27	2.22 ± 0.28	2.20 ± 0.28
	34.	TR	1.45 ± 0.23	1.46 ± 0.24	1.43 ± 0.25
	35.	RAM	17.66 ± 2.05	17.71 ± 2.59	17.60 ± 1.44
	Foramen diameters and foramen-related measurements	36.	OCHW	6.84 ± 1.33	6.806 ± 1.04
37.		FMH	5.23 ± 0.59	5.30 ± 0.60	5.16 ± 0.63
38.		FMW	6.10 ± 0.47	6.128 ± 0.59	6.06 ± 0.38
39.		FMI	85.75 ± 6.57	86.59 ± 7.73	84.92 ± 5.95
40.		RMF	0.67 ± 0.21	0.65 ± 0.22	0.68 ± 0.23
41.		IRMF	1.58 ± 0.47	1.45 ± 0.48	1.74 ± 0.46
42.		MFCB	6.21 ± 2.10	6.53 ± 2.53	5.82 ± 1.65
43.		MFMF	29.27 ± 1.96	29.60 ± 1.27	28.88 ± 2.68
44.		MFMB	4.24 ± 0.69	4.22 ± 0.35	4.27 ± 1.02
45.		MFCP	14.04 ± 0.99	14.47 ± 0.75	13.53 ± 1.07
46.		IFMO	1.45 ± 0.41	1.35 ± 0.33	1.60 ± 0.51
47.		IFP	6.19 ± 1.57	6.43 ± 0.92	5.84 ± 2.40
48.		FCIF	14.70 ± 2.75	14.58 ± 2.86	14.90 ± 2.99
49.		ZPIF	17.45 ± 2.17	16.99 ± 2.17	18.14 ± 2.30
50.		DIF	1.01 ± 0.19	1.048 ± 0.21	0.96 ± 0.17
51.		DIC	1.17 ± 0.23	1.14 ± 0.25	1.21 ± 0.22
52.		ICMC	1.62 ± 0.60	1.53 ± 0.66	1.72 ± 0.57

A mid-sagittal cut of the skull was made to reveal the neurocranium. The frontal sinus appeared to be limited only to the cranial aspect of the bone and was very small, appearing like pin-point holes, probably due to the thinness of the bones of the skull. The neurocranial cavity was relatively smooth; revealing few impressions of corresponding gyri and sulci from the brain (Figure 5).

Major morphological differences observed between the skulls of the two regions were:

1. The bat skulls from Jos (northern Nigeria) had a distinct dome-shape, formed by the parietal bone, unlike the bats from the south which had a flattened shape (Figure 1), making the southern skulls appear longer.
2. The zygomatic process emanating laterally (and projecting latero-ventrally) from the frontal bone was conspicuously more pronounced in the northern skulls, in some cases, twice as long as in the southern skulls (Figure 2).

Table 2:

Linear morphometric values of *Eidolon helvum* skulls from the northern region (Jos) compared to the southern region (Ibadan) of Nigeria, with gender-based values

S/N	Parameters (unit – mm)	Jos (northern Nigeria)			Ibadan (southern Nigeria)		
		Mean ± S.D. n = 7	Mean ± S.D. (Male) n = 4	Mean ± S.D. (Female) n = 3	Mean ± S.D. n = 12	Mean ± S.D. (Male) n = 6	Mean ± S.D. (Female) n = 6
Neurocranial and viscerocranial measurements							
1.	WSH	25.32 ± 0.66	24.99 ± 0.42	25.77 ± 0.73	21.75 ± 1.43	22.66 ± 0.74	20.85 ± 1.52
2.	WSL	55.65 ± 1.11*	55.47 ± 1.04	55.88 ± 1.40	54.88 ± 4.09	57.56 ± 0.00	53.54 ± 4.77
3.	SHWM1	19.08 ± 0.73	18.71 ± 0.50	19.58 ± 0.75	12.45 ± 0.93	11.59 ± 0.00	12.88 ± 0.80
4.	MWS	32.92 ± 0.86	32.35 ± 0.41	33.67 ± 0.67	27.01 ± 1.41	27.66 ± 1.17	26.37 ± 1.70
5.	FBL	20.24 ± 1.44	20.72 ± 1.41	19.60 ± 1.48	16.28 ± 1.43	15.42 ± 1.34	17.14 ± 1.19
6.	NBL	22.34 ± 1.57#	21.52 ± 1.63	23.44 ± 0.49	26.97 ± 3.80	30.01 ± 0.67	23.93 ± 2.43
7.	FNE	17.39 ± 1.22	16.90 ± 1.42	18.03 ± 0.56	12.99 ± 0.59	12.70 ± 0.67	13.28 ± 0.50
8.	PAL	28.74 ± 1.03 ^β	28.64 ± 0.79	28.87 ± 1.49	35.79 ± 3.24	37.79 ± 1.03	33.78 ± 3.78
9.	UMP	4.17 ± 0.37	4.28 ± 0.40	4.040 ± 0.35	1.87 ± 0.56	1.59 ± 0.40	2.420 ± 0.00
10.	TBL	3.73 ± 0.30	3.67 ± 0.16	3.81 ± 0.46	3.30 ± 0.12	3.19 ± 0.00	3.36 ± 0.11
11.	TBW	3.10 ± 0.25	2.97 ± 0.09	3.29 ± 0.29	2.80 ± 0.22	2.94 ± 0.00	2.67 ± 0.28
12.	OVD	12.67 ± 0.26	12.69 ± 0.22	12.64 ± 0.34	10.33 ± 1.02	10.75 ± 0.14	9.90 ± 1.54
13.	OHD	12.35 ± 0.25	12.37 ± 0.28	12.32 ± 0.26	11.07 ± 0.77	11.41 ± 0.86	10.72 ± 0.74
14.	Orbital index (%)	97.46 ± 1.38 ^β	97.46 ± 1.56	97.46 ± 1.44	107.60 ± 6.92	106.10 ± 6.63	109.00 ± 9.55
15.	Cephalic index (%)	59.18 ± 2.08	58.34 ± 1.66	60.30 ± 2.37	48.40 ± 1.77	46.61 ± 0.00	49.30 ± 1.21
16.	OCH	11.84 ± 0.55	11.71 ± 0.53	12.01 ± 0.64	8.72 ± 0.43	8.39 ± 0.00	8.89 ± 0.45
17.	OCW	10.23 ± 0.44	10.36 ± 0.50	10.06 ± 0.37	8.57 ± 0.33	8.20 ± 0.00	8.75 ± 0.14
18.	NCV (mls)	4.41 ± 0.28	4.20 ± 0.08	4.68 ± 0.13	2.0 ± 0.27	2.15 ± 0.07	1.85 ± 0.35
19.	LPO	10.46 ± 0.98	10.14 ± 0.60	10.89 ± 1.36	6.11 ± 0.72	6.62 ± 0.63	5.60 ± 0.29
20.	POPO	24.99 ± 1.29	24.23 ± 0.96	26.01 ± 0.95	18.20 ± 1.29	18.96 ± 0.00	17.83 ± 1.56
21.	POZB	5.97 ± 0.33*	5.80 ± 0.34	6.21 ± 0.07	5.55 ± 0.56	6.00 ± 0.02	5.10 ± 0.38
22.	NIL	6.68 ± 0.19*	6.72 ± 0.22	6.62 ± 0.15	6.45 ± 0.31	6.49 ± 0.40	6.40 ± 0.34
Mandibular measurements							
23.	MDL	43.81 ± 1.09#	43.44 ± 0.81	44.30 ± 1.39	46.19 ± 3.86	48.11 ± 1.02	44.27 ± 5.38
24.	MDL-1	41.32 ± 0.87#	41.45 ± 0.46	41.14 ± 1.37	42.04 ± 3.57	43.71 ± 0.80	40.38 ± 5.15
25.	MDL-2	41.37 ± 1.37#	40.66 ± 0.71	42.31 ± 1.60	45.33 ± 4.08	47.34 ± 1.15	43.33 ± 5.71
26.	MDL-3	40.23 ± 1.01#	39.80 ± 0.76	40.80 ± 1.14	43.13 ± 3.37	44.93 ± 1.97	41.33 ± 4.15
27.	HSPH	4.61 ± 0.44*	4.56 ± 0.34	4.68 ± 0.62	4.45 ± 0.51	4.63 ± 0.44	4.28 ± 0.69
28.	LSPH	6.71 ± 0.52	6.85 ± 0.69	6.53 ± 0.13	5.30 ± 0.34	5.59 ± 0.02	5.01 ± 0.12
29.	WCP	5.12 ± 0.21	4.99 ± 0.12	5.29 ± 0.16	4.41 ± 0.35	4.61 ± 0.15	4.22 ± 0.45
30.	D2P	6.69 ± 0.40#	6.63 ± 0.51	6.76 ± 0.26	7.22 ± 0.53	7.41 ± 0.19	7.03 ± 0.81
31.	DLM	14.65 ± 0.82	14.32 ± 0.57	15.09 ± 1.00	11.69 ± 1.07	12.15 ± 0.56	11.24 ± 1.51
32.	HMP	4.41 ± 0.26#	4.42 ± 0.18	4.40 ± 0.40	4.593 ± 0.48	4.75 ± 0.46	4.44 ± 0.62
33.	TM-1	2.38 ± 0.14	2.39 ± 0.12	2.37 ± 0.19	1.91 ± 0.09	1.89 ± 0.04	1.94 ± 0.13
34.	TR	1.60 ± 0.11	1.61 ± 0.05	1.58 ± 0.19	1.18 ± 0.04	1.16 ± 0.04	1.20 ± 0.01
35.	RAM	16.53 ± 0.89 ^β	16.20 ± 0.71	16.98 ± 1.03	19.63 ± 2.06	20.73 ± 2.14	18.53 ± 1.82
Foramen diameters and foramen-related measurements							
36.	OCHW	7.55 ± 0.82	7.25 ± 0.34	7.94 ± 1.19	5.193 ± 0.40	5.030 ± 0.00	5.275 ± 0.53
37.	FMH	5.54 ± 0.37	5.50 ± 0.46	5.51 ± 0.32	4.50 ± 0.06	4.48 ± 0.00	4.52 ± 0.08
38.	FMW	6.33 ± 0.31	6.34 ± 0.43	6.31 ± 0.14	5.56 ± 0.29	5.30 ± 0.00	5.69 ± 0.26
39.	FMI (%)	87.70 ± 6.55	87.11 ± 8.83	88.50 ± 3.15	81.20 ± 4.58	84.53 ± 0.00	79.54 ± 5.03
40.	RMF	0.73 ± 0.19*	0.76 ± 0.19	0.70 ± 0.23	0.55 ± 0.23	0.44 ± 0.01	0.66 ± 0.33
41.	IRMF	1.54 ± 0.28#	1.44 ± 0.31	1.67 ± 0.20	1.66 ± 0.76	1.47 ± 0.93	1.86 ± 0.84
42.	MFCB	4.94 ± 0.87 ^β	4.96 ± 0.95	4.92 ± 0.97	8.42 ± 1.73	9.66 ± 0.04	7.18 ± 1.68
43.	MFMF	29.18 ± 1.19#	29.09 ± 0.96	29.30 ± 1.67	29.44 ± 3.14	30.63 ± 1.46	28.25 ± 4.67
44.	MFMB	4.61 ± 0.47	4.40 ± 0.22	4.89 ± 0.61	3.60 ± 0.55	3.85 ± 0.26	3.35 ± 0.56
45.	MFCP	14.01 ± 0.92#	14.28 ± 0.85	13.65 ± 1.05	14.11 ± 1.25	14.86 ± 0.43	13.37 ± 1.52
46.	IFMO	1.23 ± 0.15 ^β	1.15 ± 0.15	1.34 ± 0.09	1.95 ± 0.35	1.75 ± 0.01	2.36 ± 0.00
47.	IFP	5.48 ± 1.30 ^β	5.86 ± 0.24	4.99 ± 2.08	7.84 ± 0.51	7.58 ± 0.30	8.38 ± 0.00
48.	FCIF	13.11 ± 1.09 ^β	12.86 ± 1.30	13.44 ± 0.87	18.43 ± 0.83	18.02 ± 0.59	19.25 ± 0.00
49.	ZPIF	18.62 ± 0.93	18.17 ± 0.68	19.22 ± 0.97	14.73 ± 1.68	14.64 ± 2.36	14.91 ± 0.00
50.	DIF	1.08 ± 0.17*	1.12 ± 0.24	1.04 ± 0.04	0.85 ± 0.12	0.92 ± 0.02	0.71 ± 0.00
51.	DIC	1.27 ± 0.20	1.25 ± 0.23	1.30 ± 0.19	0.99 ± 0.18	0.90 ± 0.01	1.08 ± 0.26
52.	ICMC	1.20 ± 0.16 ^β	1.11 ± 0.12	1.33 ± 0.14	2.34 ± 0.21	2.38 ± 0.06	2.31 ± 0.35

* Indicates values which were higher in Jos skulls but no statistically significant difference was observed when compared to Ibadan skulls ($p > 0.05$)

Indicates values which were higher in Ibadan skulls although no statistically significant difference was observed ($p > 0.05$)

^β Indicates values higher in Ibadan skulls, with statistically significant difference observed ($p < 0.05$)

All other values were higher in the Jos skulls with statistically significant difference observed ($p < 0.05$)

3. The frontal bone in the northern skulls extended more caudally, the crests formed by the two lateral aspects extended through the parietal bone to the occipital bone, forming a double sagittal crest (V-shaped); while in the southern skulls, the caudal aspect of the frontal bone formed a distinct divergent 'Y-shape' which demarcated the fronto-parietal suture, and continued caudally as a single crest. The sagittal crest in both skull types were distinct and pronounced (Figures 1 and 2).
4. There was the presence of a diastema in the southern skulls, unlike the northern skulls (Figure 1).
5. The nasal bone in the southern skulls had a slightly more convex appearance (Figure 2).
6. The southern skulls had a dental formula of $I^{2/2} C^{1/1} PM^{1/2} M^{2/3}$ (total 28), while the northern skulls had $I^{2/2} C^{1/1} PM^{2/2} M^{3/3}$ (total 32). (Figure 3). This finding was consistent in both genders.
7. The suture lines in the southern skulls were more distinct than the northern skulls. For example, the nasal bones showed a more distinct demarcation in the southern skulls relative to the northern skulls, where the maxillo-nasal sutures were not so apparent (Figure 2).
8. From a dorsal view, the southern skulls appeared more streamlined and narrower relative to the northern skulls (Figure 2).
9. Two of the southern skulls had accessory infraorbital foramen (Figure 6).
10. The palatine bone in the southern skull was more concave than that of the northern bone which was quite flatter (Figure 3).
11. Palatine foramen observed in northern skulls but not in southern skulls (Figure 3).

All the differences observed and stated above were consistent in all the skull specimens examined.

Morphometric results: Combined results of the skulls, without geographical segregation, showed no statistically significant differences between the sexes (Table 1).

However, analysis based on geographical location showed statistical differences among the skulls. Six (6) parameters were observed to be higher in the northern skulls with no statistically significant difference observed ($p > 0.05$) – WSL, RMF, NIL, DIF, HSPH, POZB; ten (10) values were higher in the southern skulls with no statistically significant difference observed ($p > 0.05$) – NBL, MDL, IRMF, MFMF, MFCP, MDL-1, MDL-2, MDL-3, HMP, D2P; while nine (9) parameters were higher in the southern skulls with statistically significant differences observed ($p < 0.05$) – PAL, orbital index, MFCB, RAM, IFMO, IFP, FCIF, ICMC. All other parameters were higher in the northern skulls with statistically significant differences observed ($p < 0.05$) (Table 2).

The neurocranial volume of the northern skulls was about twice that of the southern skulls, while in the southern skulls, the distance between the mandibular foramen and the caudal border of the mandible (MFCB) was almost twice that observed in the northern skulls. The southern skulls generally had longer mandibles, and the 'caudal angle' of the ramus dipped more ventrally than in the northern skulls.

Pearson's correlation coefficient to WSL revealed the highest positive correlations to lengths of mandible, MDL ($r = 0.822$), MDL-1 ($r = 0.880$), MDL-2 ($r = 0.674$), MDL-3 (r

$= 0.727$); FCIF ($r = 0.718$) and MFCP ($r = 0.712$). Highest negative correlations were observed with UMP ($r = -0.718$), ZPIF ($r = -0.676$) and the orbital index ($r = -0.640$) (Table 3).

Table 3:

Pearson's correlation coefficient values (r) relative to WSL

S/N	Parameters	r value	S/N	Parameters	r value
Neurocranial and viscerocranial measurements					
1	WSH	0.541	27	LSPH	0.243
2	SHWM1	0.041	28	WCP	0.073
3	MWS	0.299	29	D2P	0.489
4	FBL	0.333	30	DLM	0.480
5	NBL	0.539	31	HMP	0.435
6	FNE	0.078	32	TM-1	0.293
7	PAL	0.329	33	TR	0.095
8	UMP	-0.718	34	RAM	0.357
9	TBL	0.283	35	OCHW	0.292
10	TBW	0.191	Foramen diameters and foramen-related measurements		
11	OVD	0.506	36	FMH	0.104
12	OHD	0.430	37	FMW	0.297
13	Orbital index	-0.640	38	FMI (%)	-0.136
14	Cephalic index	-0.047	39	RMF	0.259
15	OCH	0.245	40	IRMF	0.453
16	OCW	0.234	41	MFCB	-0.151
17	NCV	0.298	42	MFMF	0.844
18	LPO	0.271	43	MFMB	0.553
19	POPO	0.526	44	MFCP	0.712
20	POZB	0.206	45	IFMO	0.606
21	NIL	0.264	46	IFP	0.082
22	MDL	0.822	47	FCIF	0.718
Mandibular measurements					
23	MDL-1	0.880	48	ZPIF	-0.676
24	MDL-2	0.674	49	DIF	-0.201
25	MDL-3	0.727	50	DIC	-0.268
26	HSPH	0.422	51	ICMC	0.024

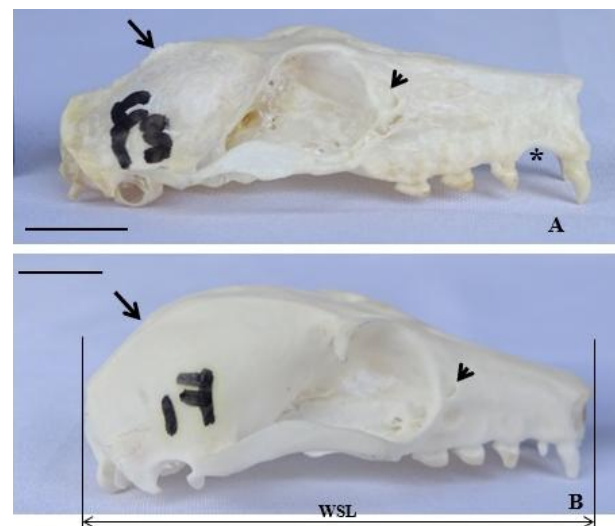


Plate 1:

Lateral view of the female *Eidolon helvum* skulls showing the external lacrimal foramen (arrow heads). A is the southern skull while B is the northern skull. Note the more pronounced external sagittal crest (arrows) and the diastema (*) in the southern skull, and the dome-shaped appearance of the northern skulls relative to the flattened appearance of the southern skulls. Note also the whole skull length (WSL). Scale bar – 1 cm.

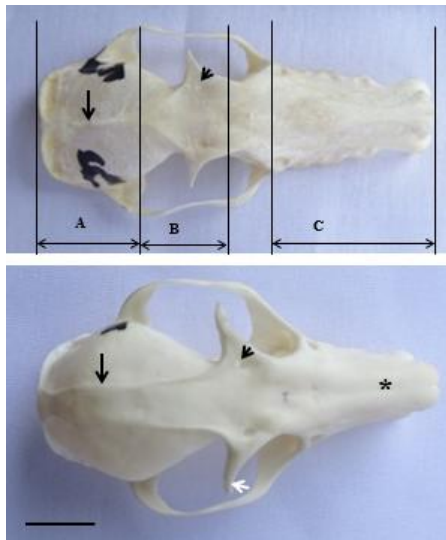


Plate 2: Dorsal view of the skull of the female *Eidolon helvum*, southern skull (top panel) and northern skull (lower panel), showing the length of the parietal bone – FNE (A), the total length of the frontal bone – FBL (B) and the overall length of the nasal bone – NBL (C). Note the supra-orbital foramen present in both skulls (arrow head), the more convex nasal bone in the southern skull relative to northern skull (*), the difference in the shapes of the external sagittal crests (arrows) and the longer zygomatic process of the frontal bone (white arrow) in the northern skull. Scale bar 1 cm.

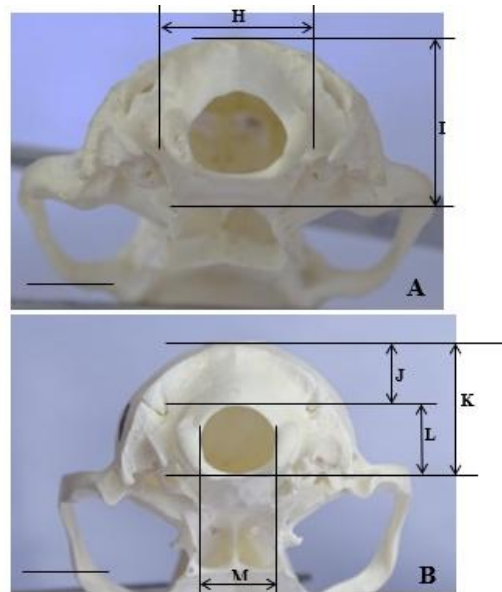


Plate 4: Occipital view of the skull of the female *Eidolon helvum*, A – southern skull, B – northern skull. Pictures show the maximum width of the occipital condyles – OCW (H); skull height without mandible 1 – SHWM-1 (I); occipital height without foramen magnum – OCHW (J); occipital height – OCH (K); height of the foramen magnum – FMH (L); and width of the foramen magnum – FMW (M). Scale bar 1 cm.

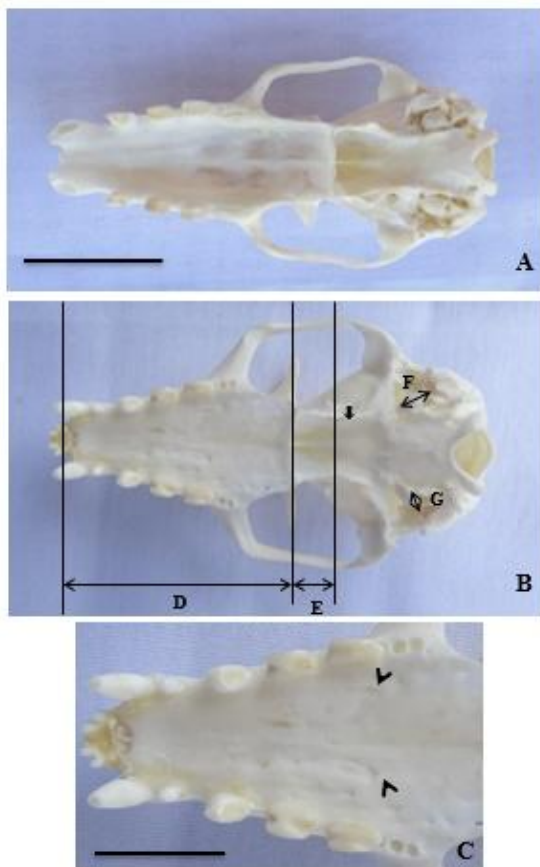


Plate 3: Ventral view skull of the female *Eidolon helvum*. A – southern skull, B – northern skull. Note – length of the palate, PAL (D); the length of the perpendicular plate of the palatine bone, UMP (E); length of the tympanic bulla, TBL (F); width of the tympanic bulla, TBW (G). Arrow indicates the hamulus of the pterygoid bone. Note the more pronounced concavity of the southern skull (A), the absence of palatine fissure or inter-incisive canal on the 2 skulls, the variation in dentition and the presence of the palatine foramen on the northern skull (arrow heads on panel C). C is magnification of palatine bone of B (northern skull). Scale bar – 2 cm (A & B), 1 cm (C).

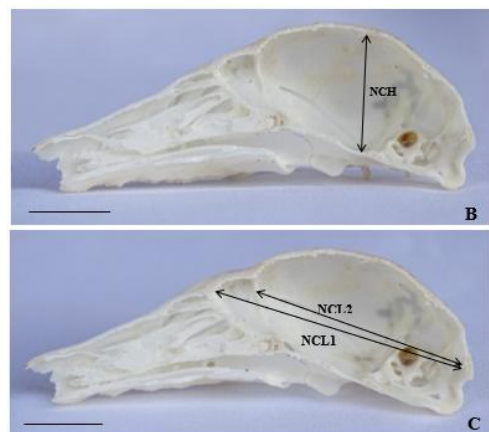
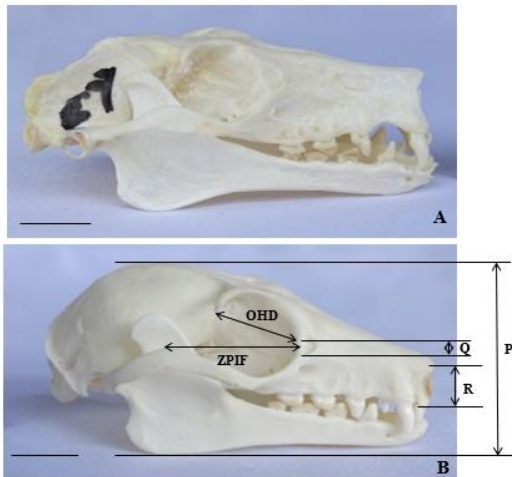


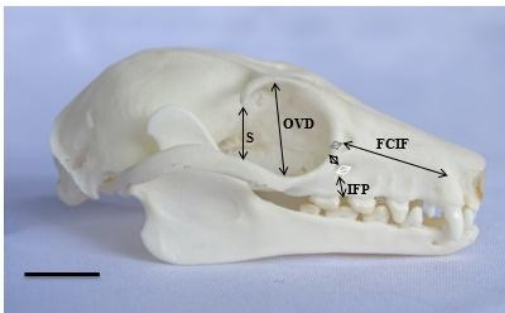
Plate 5: Medial view of the neurocranium of the female *Eidolon helvum*, showing the neurocranial height – NCH; neurocranial length with the ethmoid fossa – NCL1 and the neurocranial length without the ethmoid fossa – NCL2. Scale bar 1 cm



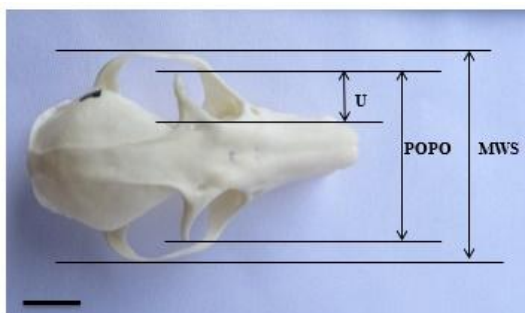
Plate 6: Lateral and rostro-lateral views of the *Eidolon helvum* southern skull. Note the lacrimal foramen (arrow) and the infraorbital foramen and accessory (arrow heads).

**Plate 7:**

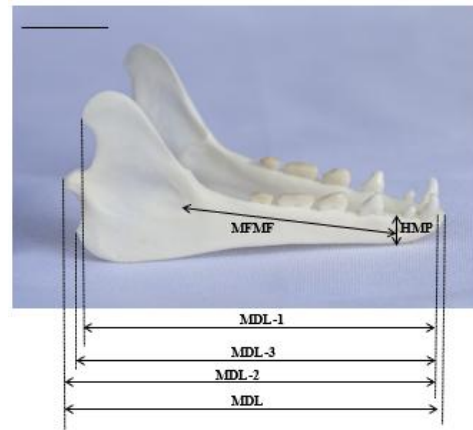
Lateral view of the skull (northern) of the female *Eidolon helvum*, showing the whole skull height – WSH (P); the horizontal diameter of the orbit – OHD; the distance from the zygomatic arch to the caudal rim of the infra-orbital foramen – ZPIF; the diameter of the lacrimal foramen – DIF (Q) and the distance from the rostral tip of the nasal bone to the rostral tip of the incisive bone – NIL (R). A – southern skull, B – northern skull; note the similarity in the dentition of the lower jaw (lower first premolar and canine missing in southern skull). Scale bar 1 cm.

**Plate 8:**

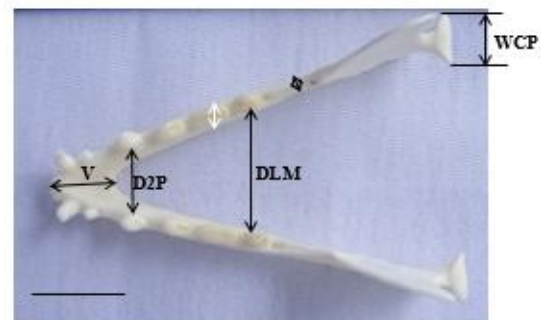
Lateral view of the skull of the female *Eidolon helvum*, showing the vertical diameter of the orbit – OVD, the vertical distance from the most lateral limit of postorbital process to zygomatic bone – POZB (S), the distance, along a horizontal line, between the caudal rim of the lacrimal foramen and the cranial tip of the facial crest – FCIF, the distance from the ventral limit of the infraorbital foramen to the alveolar border between the upper 3rd and 4th premolars – IFP, the distance between the infraorbital foramen and the median canthus of the orbit/the orbit – ICMC (black arrow), the diameter of the infraorbital foramen – DIC (white arrow), and the distance between the caudal limit/rim of the lacrimal foramen and the medial canthus of the orbit – IFMO (grey arrow). Scale bar 1 cm.

**Plate 9:**

Dorsal view of the skull of the female *Eidolon helvum*, showing the maximum width of the skull, MWS; the length of the zygomatic process of the frontal bone, LPO (U); and the distance from one limit of the zygomatic process to the other, POPO. Scale bar 1 cm.

**Figure 10:**

Lateral view of the mandible of the female *Eidolon helvum*, showing the height of the mandibular body from the mid-point of premolar 1 and 2 to the mandibular base, HMP; the length, along a vertical line, from the ventral limit of the middle mental foramen, to the ventral border of the mandibular foramen, MFMF; the length of the lower jaw from the most rostral point of the dental bone to the most caudal projection of the coronoid process, MDL-1; the length of the lower jaw from the most rostral point of the dental bone to the most caudal projection of the mandibular condyle (condylar process), MDL-2; the length of the lower jaw, from the most rostral point of the dental bone to the most caudal projection of the angular process, MDL-3; and the length of the mandibular bone, MDL. Scale bar 1 cm.

**Figure 11:**

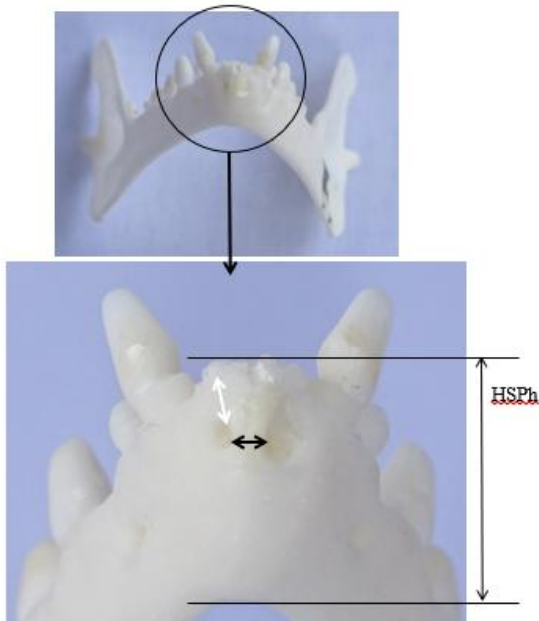
Dorsal view of the mandible of the female *Eidolon helvum*, showing the length of the mandibular symphysis, LSPh (V); the distance between the two lower (mandibular) premolars, at the level of the 2nd premolars, measured along the transverse plane, D2P; the distance between the lower (mandibular) 2nd molars, measured along the transverse plane, DLM; the thickness of mandible at molar 1, TM-1 (white arrow); the thickness of the mandible, between the medial and lateral parts of the mandible, caudal to the last molar tooth, TR (black arrow); and the width of the condylar process, WCP. Scale bar 1 cm.

DISCUSSION

Skull variation in size and shape has been reported among different species of mammals, example, the gray wolf (Milenković *et al.*, 2010), but has been reported to occur more in dogs, with skull shapes varying from dolichocephalic, brachycephalic to mesaticephalic (Drake and Klingenberg, 2010; Janeczek *et al.*, 2008; Onar and Günes, 2003). Bat skulls have been documented to show variations in shape, differing from species to species (Brokaw and Smotherman, 2020; Camacho *et al.*, 2019; Freeman, 1998, 2000; Pedersen, 1995). But so far, no documentation on skull variations within bat species could be ascertained at the time of this write-up. The two skull types showed a distinct dolichocephalic appearance, consistent with previous pictorial reports in the *E helvum* (DeFrees and Wilson, 1988).

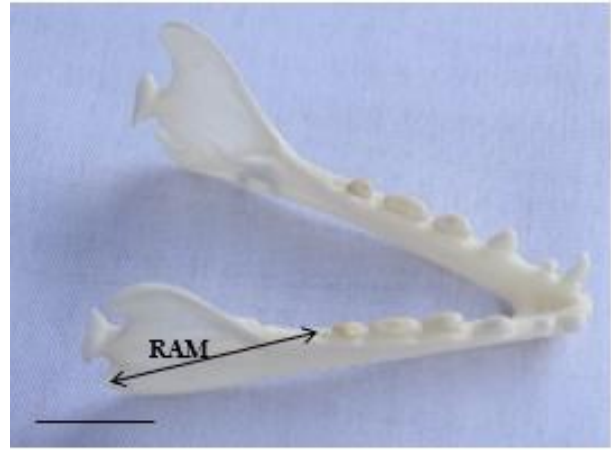
**Figure 12:**

Caudo-lateral view of the mandible of the female *Eidolon helvum*, showing the distance between the ventral limit of the mandibular foramen and the caudal border of the mandible, MFCB (X); the mandibular foramen to the base of the mandible, MFMB (W); the ventral limit of the mandibular foramen to the most dorsal aspect of the coronoid process, MFCP (Y). Scale bar 1 cm.

**Figure 13:**

Rostral view of the mandible of the female *Eidolon helvum*, showing the distance between the most medial points of the most rostral left and right mental foramina, RMF (black arrow); the distance between the alveolar border of the 2nd incisor and the rostral mental foramen, IRMF (white arrow); and the height of the mandibular symphysis – HSPh.

The zygomatic process of the frontal bone, emanating from the dorso-lateral aspect, was observed to be more pronounced than that observed in dogs. Not all animals have this process, e.g. the equine; but in some of those that possess it (like the dog, cat, porcine) the supraorbital foramen on its dorsal aspect is absent. The foramen has however been reported to be present in ruminants (Getty, 1975; Singh, 2017). Unlike the cat however, the bats lack the frontal process of the zygomatic bone, which is directed dorsally, emanating from the zygomatic arch (Getty, 1975; Singh, 2017). The frontal bone accommodates the frontalis muscle and some other muscles controlling the movements of the eyelids and the nasal region. The prominence of the zygomatic process may indicate that some of these muscles are stronger or bigger in these species. The supraorbital foramen houses the supraorbital nerve which innervates the upper eyelid and the adjacent parts of the skin of the forehead (Singh, 2017).

**Figure 14:**

Dorso-lateral view of the mandible of the female *Eidolon helvum*, showing the length of the mandible from the angular process to the last molar tooth, RAM. Scale bar 1 cm.

The sagittal crest is usually described as a ridge of bone, on the dorsal and midline aspect of the skull, running lengthwise. It has been observed in the skulls of mammals and reptiles and functions for muscle attachment (Igado, 2017; Igado *et al.*, 2015; Singh, 2017). This crest accommodates and serves as attachment for some muscles of mastication (Getty, 1975; Singh, 2017), therefore, the difference in shape of the sagittal crests observed could indicate a difference or adaptation in eating and chewing pattern, based on geographical location.

Previous pictorial reports on the skull of the *Eidolon helvum* show a more dome-shaped appearance, similar to that observed in the northern skulls (DeFrees and Wilson, 1988). The dome shape observed in the northern skulls could probably indicate that the brains of these animals were relatively bigger than the southern skulls. This dome shape was mainly due to the more convex shape of the frontal, parietal and occipital bones, which are the dorsal bones of the neurocranium (Singh, 2017). This hypothesis of the northern brains being bigger is also supported by the fact that the neurocranial volume in the northern skulls was statistically significantly higher than that of the southern skulls. The relatively smooth inner surface of the skull in both skull types is reflected in the lissencephalic nature of the brain (Igado *et al.*, 2012), as the presence of gyri results in corresponding grooves on surface of the neurocranium. Further research may reveal the differences in the brain size and also general neuro-architecture.

In the mammalian embryo, teeth development is through a number of interactions between the “odontogenic epithelium and the neural crest-derived ectomesenchyme of the early jaw primordia” (Cobourne and Sharpe, 2010). Intra-species variation in dentition has been reported in the Ipanema bat (Dick, 2002), and also in the *Eidolon helvum* (Igado *et al.*, 2018). These variations in dentition were due to differences in the number of the cheek teeth. Interestingly, the *Eidolon helvum* were obtained from the southern part of Nigeria, but in a different state from that used in the current study. The study reported differences between the genders, with the males have 30 to 36 teeth in total, and the females having 30 to 34. The reasons for the fact that no differences were observed in the dentition by the current authors could possibly be due to the number of bats used. The diastema observed in the southern skulls could

also contribute to the reduction in the number of teeth relative to the northern skulls.

As reported in domestic dogs, variation in the skull shape has been reported to have obvious functional consequences, for example on the force of bite and on breathing (Drake and Klingenberg, 2010). The shape of the external nares and its orientation are probably involved in the control of airflow into the nasal cavity for the purposes of olfaction and respiration (Clifford and Witmer, 2004; Craven *et al.*, 2007; Ranslow *et al.*, 2014) Nasal shape variation has been reported generally in bats, differing from species to species. This variation in nasal shape and other facial features has been reported to correlate with feeding ecology and echolocation (Brokaw and Smotherman, 2020), however in this study, the two groups of bats used were of the same species, having the same fruit diet. Morphological adaptations of the nose also improve the ability to detect and track odours, an essential aspect of animal survival. While odour detection may be enhanced by increased nostril separation (Brokaw and Smotherman, 2020) (an aspect which was not explored in this study), the slightly more convex appearance in the southern skulls may indicate an increased nostril separation, probably implying their possession of a keener sense of smell.

The palatine bone showed distinct differences – more concave in the southern skulls coupled with the presence of the palatine foramen. The presence of the palatine foramen may make some dental and oral anaesthesiology easier in surgical interventions and examinations. The long and narrow shape of the palate and fused mandibular symphysis are consistent with reports by Freeman (Freeman, 1998) on observations in other species of frugivorous megachiropterans. The fused mandibular symphysis helps to stabilise and strengthen the rostral aspect of the jaw (Freeman, 1998). The differences observed in the palatine bone and the distinctiveness of the suture lines may be attributed to changes in the development of the cranium resulting in modifications of the skull or the whole skeleton (Camacho *et al.*, 2019).

Some reports have been documented of variation in skull shape and size in breeds of animals obtained from different geographical locations, for example, Rodent *Ctenomys* (Fernandes *et al.*, 2009), the gray wolf (Milenković *et al.*, 2010), domestic dogs (Drake and Klingenberg, 2010) and based also on the racial variations in humans (Durbar, 2014). In spite of the fact that the bats used in this study were all phenotypically *Eidolon helvum*, the results obtained from this study indicate the possibility of an ecology-based variation. In addition, since bats are animals that migrate over long distances (DeFrees and Wilson, 1988), these skull differences may also indicate an adaptation for survival based on the distances travelled and the peculiarities of the geographical locations. In humans, craniometry has been used to determine the race and sex of the subject (Durbar, 2014). It remains to be seen if this can be applied completely to bats, although in this study, results obtained show that measurements alone may not be sufficient to distinguish males from females.

In conclusion, the *Eidolon helvum* still remains one of the most common frugivorous bats in Nigeria. These distinct variations in skull features based on location may shed more light on the effect of ecology on skeletal morphology, and may act as a guide when handling these species, most

especially in clinical and surgical manoeuvres. This report is probably the first documenting skull shape variation in the *E. helvum* obtained from different locations in the same country.

Acknowledgements

The authors gratefully acknowledge the assistance of Dr. T. B. Joannis of the Nigerian Veterinary Research Institute (NVRI), Jos, Plateau State, in capturing the bats from the north (Jos) and also Mr. A.W. Ramoni, of Veterinary Anatomy Department, University of Ibadan for his technical assistance in the maceration.

Author contributions

OOI: Conceptualization, data curation, formal analysis, investigation, methodology, project administration, resources, software, supervision, validation, manuscript draft, review and editing.

JSJ: Data curation, formal analysis, investigation, methodology, manuscript draft.

REFERENCES

- Balthazary, S. T., Max, R. ., Mlay, E., Shayo, G., Mlay, P., and Phiri, E. C. J. H. (2007) Some haematological, biochemical and zootechnical parameters of fruit eating bat (*Eidolon helvum*) in Morogoro Tanzania. *Tanzania Veterinary Journal* 24: 129–138.
- Brokaw, A. F., and Smotherman, M. (2020) Role of ecology in shaping external nasal morphology in bats and implications for olfactory tracking. *PLoS ONE* 15(1): 1–22.
- Bullen, R. D., and McKenzie, N. L. (2008) Aerodynamic cleanliness in bats. *Australian Journal of Zoology* (56): 281–296.
- Camacho, J., Heyde, A., Bhullar, B. S., Haelewaters, D., Simmons, N. B., and Abzhanov, A. (2019) Peramorphosis , an evolutionary developmental mechanism in neotropical bat skull diversity. *Developmental Dynamics* 248(June): 1129–1143.
- Clifford, A. B., and Witmer, L. M. (2004) Case studies in novel narial anatomy: 2. The enigmatic nose of moose (*Artiodactyla: Cervidae: Alces alces*). *J. Zool.* 262: 339–360.
- Cobourne, M. T., and Sharpe, P. T. (2010) Making up the numbers: The molecular control of mammalian dental formula. *Seminars in Cell and Developmental Biology* 21(1): 314–324.
- Craven, B. A., Neuberger, T., Paterson, E. G., Webb, A. G., Josephson, E. M., Morrison, E. E., and Al., E. (2007) Reconstruction and morphometric analysis of the nasal airway of the dog (*Canis familiaris*) and implications regarding olfactory airflow. *Anatomical Record* 290: 1325–1340.
- DeFrees, S. I., and Wilson, D. E. (1988) *Eidolon helvum*. *Mammalian Species* 312: 1–5.
- Dick, C. W. (2002) Variation in the dental formula of the ipanema bat, *Pygoderma bilabiatum*. *Southwestern Naturalist* 47(3): 505–508.
- Drake, A. G., and Klingenberg, C. P. (2010) Large-Scale Diversification of Skull Shape in Domestic Dogs : Disparity and Modularity. *The American Naturalist* 175(3): 289–301.
- Durbar, U. S. (2014) Racial Variations in Different Skulls. *Journal of Pharmaceutical Sciences and Research* 6(11): 370–372.
- Fernandes, F. A., Fornel, R., Cordeiro-estrela, P., and Freitas, T. R. O. (2009) Intra- and interspecific skull variation in two sister species of the subterranean rodent genus *Ctenomys*

- (Rodentia, Ctenomyidae): coupling geometric morphometrics and chromosomal polymorphism. *Zoological Journal of the Linnean Society* 155: 220–237.
- Freeman, P. W. (1998) Form, Function, and Evolution in Skulls and Teeth of Bats. *Papers in Natural Resources*. Paper 9.
- Freeman, P. W. (2000) Macroevolution in Microchiroptera: Recoupling morphology and ecology with phylogeny. *Evolutionary Ecology Research* 2(3): 317–335.
- Getty, R. (1975) *The Anatomy of the Domestic Animals*, Vol 1 & 2, 5th edn. Philadelphia, PA: Saunders Company.
- Gibson, L., Ribas, M. P., Kemp, J., Restif, O., Suu-ire, R. D., Wood, J. L. N., and Cunningham, A. A. (2021) Persistence of Multiple Paramyxoviruses in a Closed Captive Colony of Fruit Bats (*Eidolon helvum*). *Viruses* 13: 1–12.
- Igado, O., Femi-Akinlosotu, O., Omobowale, T., Ajadi, R., and Nottidge, H. (2018) Dental formula and dental abnormalities observed in the *Eidolon helvum* (Fruit bat) captured from the wild. *African Journal of Biomedical Research* 21(1): 223–225.
- Igado, O.O. (2017) Skull Typology and Morphometrics of the Nigerian Local Dog (*Canis lupus familiaris*). *Nigerian Journal of Physiological Sciences* 32: 153–158.
- Igado, O.O., and Ade-Julius, E. R. (2018) Gross Description and Osteometrics of the Axial Skeleton (Ribs and Vertebrae) of *Eidolon Helvum* (African Fruit Bat). *Nigerian Journal of Physiological Sciences* 33: 189–194.
- Igado, O.O., and Ekeolu, O. K. (2014) Morphometric investigation of the occipital area of the adult Nigerian Local Dogs. *African Journal of Biomedical Research* 17: 125–128.
- Igado, O.O., Olukole, S. G., Olopade, J. O., and Oke, B. O. (2015) Cranial morphometry of the African Sideneck Turtle (*Pelusios castaneus*). *Journal of Zoological and Bioscience Research* 2(3): 25–32.
- Igado, Olumayowa O, Omobowale, T. O., Ajadi, R. A., and Nottidge, H. O. (2012) Craniofacial morphometrics and macro-neurometrics of the fruit bat (*Eidolon helvum*). *European Journal of Anatomy* 16(3): 172–176.
- Janeczek, M., Chrószcz, A., Onar, V., Pazvant, G., and Pospieszny, N. (2008) Morphological Analysis of the Foramen Magnum of Dogs from the Iron Age. *Anatomia Histologia Embryologia* 37(5): 359–361.
- Juste, J., Ibanez, C., and Machordom, A. (2000) Morphological and allozyme variation of *Eidolon helvum* (Mammalia: Megachiroptera) in the islands of the Gulf of Guinea. *Biological Journal of the Linnean Society* 71: 359–378.
- Milenković, M. V. J., Šipetić, J., Blagojević, S., Tatović, and Vujošević, M. (2010) Skull variation in Dinaric–Balkan and Carpathian gray wolf populations revealed by geometric morphometric approaches. *Journal of Mammalogy* 91(2): 376–386.
- Olopade, J. O., and Onwuka, S. K. (2004) Morphometric studies of the cranio-facial region of the West African dwarf goat in Nigeria. *International Journal of Morphology* 22(2): 145–148.
- Onar, V. (1999) A morphometric study on the skull of the German shepherd dog (Alsatian). *Anat. Histol. Embryol.* 28: 253–256.
- Onar, V., and Günes, H. (2003) On the variability of skull shape in German shepherd (Alsatian) puppies. *The Anatomical Record Part A: Discoveries in Molecular, Cellular, and Evolutionary Biology* 272A(1): 460–466.
- Pedersen, S. C. (1995) Cephalometric correlates of echolocation in the chiroptera: II. Fetal development. *Journal of Morphology* 225(1): 107–123.
- Ranslow, A. N., Richter, J. P., Neuberger, T., Van Valkenburgh, B., Rumble, C. R., Quigley, A. P., and Al., E. (2014) Reconstruction and Morphometric Analysis of the Nasal Airway of the White-Tailed Deer (*Odocoileus virginianus*) and Implications Regarding Respiratory and Olfactory Airflow. *Anatomical Record* 297: 2138–2147.
- Richter, H. V., and Cumming, G. S. (2006) Food availability and annual migration of the straw-colored fruit bat (*Eidolon helvum*). *Journal of Zoology* 268: 35–44.
- Singh, B. (2017) *Dyce, Sack and Wensing's Textbook of Veterinary Anatomy*. 5th edition. Saunders, Elsevier.
- Sohayati, A. R., Zaini, C. M., Hassan, L., Epstein, J., Siti Suri, A., Daszak, P., and Sharifah, S. H. (2008) Ketamine and xylazine combinations for short-term immobilization of wild variable flying foxes (*Pteropus hypomelanus*). *Journal of Zoo and Wildlife Medicine* 39(4): 674–676.